Chebyshev collocation spectral approach for combined radiation and conduction heat transfer in one-dimensional semitransparent medium with graded index

Ya-Song Sun, Ben-Wen Li [*]

Key Laboratory of National Education Ministry for Electromagnetic Processing of Materials, P.O. Box 314, Northeastern University, Shenyang 110004, China

ARTICLE INFO

ABSTRACT

The Chebyshev collocation spectral method for discrete ordinates equation is presented to solve combined radiation and conduction heat transfer problem in semitransparent graded index media. The angular dependence of the problem is discretized by discrete ordinates method, and the space dependence is expressed by Chebyshev polynomial and discretized by collocation spectral method. The exponential convergence characteristic of the spectral methods is studied. The comparisons between the present results and those available in references indicate that, the Chebyshev collocation spectral-discrete ordinates method (SP-DOM so called) for combined radiation and conduction heat transfer in one-dimensional semitransparent medium with graded index is accurate and efficient.

© 2009 Elsevier Ltd. All rights reserved.

1. Introduction

Combined radiation and conduction heat transfer in graded index media exists in many engineering applications [1]. These applications include, for example, the analysis of heat transfer process in glasses and thermal protecting coatings, the optical measurement of flame, and so on. Because the ray goes along a curved path determined by Fermat principle [2,3], the solutions of combined radiation and conduction heat transfer in graded index (in other words, variable spatial refractive index) are more difficult than those in uniform index.

Various approximate and numerical methods have been developed for combined radiation and conduction heat transfer in the semitransparent media with graded index. In the early 1993, for radiative heat transfer in semitransparent graded index medium, Siegel and Spuckler [4] developed a model of one-dimensional composite medium made of several sublayers, each of them being treated as a slab at uniform index bounded by diffuse surfaces.

Up to now, many numerical methods have been proposed to solve the combined radiation and conduction heat transfer in graded index medium. For example, Ben Abdallah and Le Dez [5] presented a curved ray tracing method. Xia et al. [6] and Huang [7,8] proposed a combined curved ray tracing and pseudo-source adding method. Liu et al. [9] developed a discrete curved ray tracing method, later Liu and his other coworkers [10] employed a meshless local Petrov–Galerkin (MLPG) approach. In Ref. [10], even the cases of linear and sinusoidal spatial variable refractive indices were considered. Yi et al. [11] analyzed the effects of variable

refractive index on steady and transient heat transfer inside a scattering semitransparent slab. Recently, Tan et al. [12] proposed a discrete curved ray-tracing method to solve transient combined heat transfer in a semitransparent medium with graded index.

In the community of numerical simulations, it is well known that the spectral methods can provide exponential convergence (in other words, spectral accuracy) [13], and have been widely applied in computational fluid dynamics [14,15], electrodynamics [16], and magnetohydrodynamics [17]. While early in 1992, Zenouzi and Yener [18,19] used the Galerkin method to solve the radiative part of a radiation and natural convection combined problem; later Kuo et al. [20,21] made a numerical comparison for spectral methods and finite volume method to solve the radiation and natural convection combined problem, and they concluded that the spectral methods are more accurate; Ganz et al. [22] used spectral methods for radiative heat transfer in a reacting flow; De Oliveira et al. [23] made a combination of spectral method and Laplace transform to solve radiative heat transfer in an isotropic scattering media; last year, the collocation spectral method for radiative part in stellar modeling was carried out [24]; very recently, in Modest and Singh's work [25], the spherical harmonics method (P_N method so called, from mathematical view, the P_N method belongs to the category of spectral methods) was further developed to reduce the number of first-order partial differential equations.

Another four works regarding radiative transfer are the references [26–29]. However, all these four works are not really correlated with "heat transfer" by thermal radiation but with quantum physics [26], electromagnetic wave [27,28] and beam wave [29] propagation and scattering. Besides this fact, their final resultant algebraic equations need to be solved are in coefficient space, in

* Corresponding author. Tel.: +86 24 83681756; fax: +86 24 83681758.
E-mail addresses: heatli@hotmail.com, heatli@epm.neu.edu.cn (B.-W. Li).

Nomenclature

A	matrix defined in Eq. (24)
B	matrix defined in Eq. (24)
$\mathbf{D}_s^{(1)}$	the first order derivative matrix
$\mathbf{D}_s^{(2)}$	the second order derivative matrix
F	matrix defined in Eq. (24)
h_j	function of the first order derivative of Chebyshev polynomial
I	radiative intensity (W m^{-2} sr^{-1})
I_b	blackbody radiative intensity (W m^{-2} sr^{-1})
k_a	absorption coefficient (m^{-1})
k_s	scattering coefficient (m^{-1})
L	slab thickness (m)
M	the direction number
n	refractive index
N	total number of solution nodes
N_{cr}	conduction–radiation parameter
P	matrix defined in Eq. (26)
s	standard Guass–Lobatto points (m)
T	temperature (K)
T_k	the first kind Chebyshev polynomial
T_{ref}	reference temperature (K)
V	matrix defined in Eq. (26)
w^m	weight corresponding to the direction m
x	axial coordinate (m)
X	dimensionless axial coordinate

Greek symbols

α	coefficient defined in Eq. (7)
β	extinction coefficient (m^{-1})

γ	dimensionless derivative of refractive index
γ'	derivative of refractive index (m^{-1})
ϵ	wall emissivity
Θ	dimensionless temperature
$\hat{\Theta}$	coefficients for spectral approximation in Eq. (21)
κ	thermal conductivity (W m^{-1} K^{-1})
μ	direction cosines
σ	Stefan–Boltzmann constant (W m^{-2} K^{-4})
τ_L	optical thickness
Φ	scattering phase function
ψ	dimensionless radiative intensity
$\hat{\psi}$	coefficients for spectral approximation in Eq. (20)
Ψ	dimensionless radiative heat flux
ω	scattering albedo

Subscripts

0	value at $x=0$
L	value at $x=L$
i,j,k	solution node index

Superscripts

$m, m'm \pm 1/2$	angular direction of radiation
$*$	the last iterative value

another word, spectral equations. Recently, for radiative and conductive heat transfer in concentric spherical and cylindrical media with uniform index, Aouled-Dlala et al. [30] have proposed the finite Chebyshev transform (FCT) to treat the angular derivative terms in cylindrical and spherical systems. Now, Li et al. [31] have developed the Chebyshev collocation spectral method for one-dimensional radiative heat transfer even with anisotropic space dependent scattering medium with uniform index; Sun and Li [32] have presented this method to solve radiative heat transfer special in one-dimensional graded index medium; Li et al. [33] have proposed this method to solve coupled radiation and conduction in a concentric spherical participating medium.

In this paper, we extend the Chebyshev collocation spectral method to solve the combined radiation and conduction heat transfer problems in a one-dimensional semitransparent slab with graded index. In the following sections, firstly, the SP-DOM formulations for conduction–radiation heat transfer with graded index are presented. Secondly, in order to validate the SP-DOM method, some representative results are compared with those available in the literatures. Finally, conclusions are given.

2. Formulations

The considered problem is of a combined radiation and conduction heat transfer in a one-dimensional semitransparent gray slab with thickness L bounded by two opaque, diffuse and gray walls (see Fig. 1). The refractive index $n(x)$ varies along the axis coordinate x. Other optical properties such as extinction coefficient β and scattering albedo ω are assumed to be constant. The thermal conductivity κ is uniform over the slab. On both sides of the slab, the emissivities are ε_0 and ε_L, and the temperatures are imposed as T_0 and T_L, respectively.

For a steady state combined radiation and conduction heat transfer, the energy equation can be written as

$$\kappa \frac{\partial^2 T}{\partial x^2} = k_a \left(4n^2 \sigma T^4 - 2\pi \int_{-1}^{1} I d\mu \right) \tag{1}$$

with boundary conditions

$$T|_{x=0} = T_0 \tag{2a}$$
$$T|_{x=L} = T_L \tag{2b}$$

The governing equation for radiative transfer in one-dimensional absorbing–emitting–scattering medium with graded index in term of radiation intensity reads [34]

$$\mu \frac{\partial I(x,\mu)}{\partial x} + \gamma' \frac{\partial}{\partial \mu}[(1-\mu^2)I(x,\mu)] + \beta I(x,\mu)$$
$$= n^2 k_a I_b + \frac{k_s}{2} \int_{-1}^{1} I(x,\mu')\Phi(\mu',\mu)\,d\mu' \quad \text{in } [0,L] \times [-1,1] \tag{3}$$

with boundary conditions

$$I(0,\mu) = \varepsilon_0 n_0^2 \frac{\sigma T_0^4}{\pi} + 2(1-\varepsilon_0) \int_{-1}^{0} I(0,\mu')|\mu'|d\mu' \quad \text{on}$$
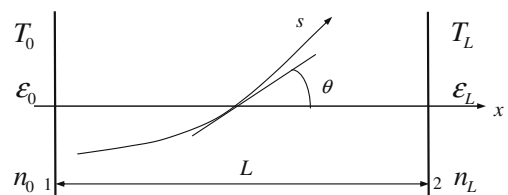$$x = 0, \ \mu \in (0,1] \tag{4a}$$

Fig. 1. Physical geometry of slab.

$$I(L, \mu) = \varepsilon_L n_L^2 \frac{\sigma T_L^4}{\pi} + 2(1 - \varepsilon_L) \int_0^1 I(L, \mu')|\mu'| d\mu' \quad \text{on}$$

$$x = L \quad \mu \in [-1, 0) \tag{4b}$$

where $\gamma' = \frac{1}{n}\frac{dn}{dx}$ is the derivative of refractive index.

The discrete form of the radiative transfer equation is obtained by evaluating Eq. (3) at each of the discrete direction and replacing the integral by numerical quadrature

$$\mu^m \frac{\partial I^m(x)}{\partial x} + \gamma' \left\{ \frac{\partial}{\partial \mu} \left[(1 - \mu^2)I(x) \right] \right\}_{\mu = \mu^m} + (k_a + k_s)I^m(x)$$

$$= n^2 k_a I_b(x) + \frac{k_s}{2} \sum_{m'=1}^M I^{m'}(x)\Phi(\mu^{m'}, \mu^m)w^{m'} \quad m = 1, 2, \ldots, M \tag{5}$$

The discrete ordinate representations of the boundary conditions, Eqs. (4a) and (4b), are given by

$$I_0^m = \frac{\varepsilon_0 n_0^2 \sigma T_0^4}{\pi} + 2(1 - \varepsilon_0) \sum_{\mu^{m'}<0} I_0^{m'}|\mu^{m'}|w^{m'} \quad \mu^m > 0 \tag{6a}$$

$$I_L^m = \frac{\varepsilon_L n_L^2 \sigma T_L^4}{\pi} + 2(1 - \varepsilon_L) \sum_{\mu^{m'}>0} I_L^{m'}|\mu^{m'}|w^{m'} \quad \mu^m < 0 \tag{6b}$$

The angular derivative term in Eq. (5) is discretized by central difference scheme, and its final form can be written as [35]

$$\left\{ \frac{\partial}{\partial \mu} \left[(1 - \mu^2)I(x) \right] \right\}_{\mu = \mu^m} \approx \frac{\alpha^{m+1/2}I^{m+1/2} - \alpha^{m-1/2}I^{m-1/2}}{w^m} \tag{7}$$

where $I^{m+1/2}$ and $I^{m-1/2}$ are the angular intensities in the directions $m + 1/2$ and $m - 1/2$, and their appropriate relations are based on the step schemes. Those are

$$\alpha^{m+1/2}I^{m+1/2} = \max\left(\alpha^{m+1/2}, 0\right)I^m - \max\left(-\alpha^{m+1/2}, 0\right)I^{m+1} \tag{8a}$$

$$\alpha^{m-1/2}I^{m-1/2} = \max\left(\alpha^{m-1/2}, 0\right)I^{m-1} - \max\left(-\alpha^{m-1/2}, 0\right)I^m \tag{8b}$$

The constants $\alpha^{m\pm1/2}$ only depend on the difference scheme and can be determined by the following recurrences:

$$\alpha^{1/2} = \alpha^{M+1/2} = 0 \tag{9a}$$

$$\alpha^{m+1/2} - \alpha^{m-1/2} = -2w^m \mu^m \tag{9b}$$

Finally, Eq. (5) can be rewritten as

$$\mu^m \frac{\partial I^m}{\partial x} + \left[\frac{\gamma'}{w^m}\max(\alpha^{m+1/2}, 0) + \frac{\gamma'}{w^m}\max\left(-\alpha^{m-1/2}, 0\right) + (k_a + k_s) \right]$$

$$I^m = \frac{\gamma'}{w^m} \left[\max\left(-\alpha^{m+1/2}, 0\right)I^{m+1} + \max(\alpha^{m-1/2}, 0)I^{m-1} \right]$$

$$+ k_a n^2 \sigma T^4 / \pi + \frac{k_s}{2} \sum_{m'=1}^M I^{m'}\Phi^{m',m}w^{m'} \tag{10}$$

For convenience of analysis, the energy equation, the discrete ordinate equation, and the corresponding boundary conditions are nondimensionalized

$$\frac{\partial^2 \Theta}{\partial X^2} = \frac{\tau_L^2}{N_{cr}}(1 - \omega)\left(n^2 \Theta^4 - \frac{1}{2} \sum_{m=1}^M \psi^m w^m \right) \tag{11}$$

$$\Theta|_{x=0} = \Theta_0 \tag{12a}$$

$$\Theta|_{x=L} = \Theta_L \tag{12b}$$

$$\frac{\mu^m}{\tau_L}\frac{\partial \psi^m}{\partial X} + \left[\frac{\gamma}{w^m}\max\left(\alpha^{m+1/2}, 0\right) + \frac{\gamma}{w^m}\max\left(-\alpha^{m-1/2}, 0\right) + 1 \right]\psi^m$$

$$= \frac{\gamma}{w^m}\max\left(-\alpha^{m+1/2}, 0\right)\psi^{m+1} + \frac{\gamma}{w^m}\max\left(\alpha^{m-1/2}, 0\right)\psi^{m-1}$$

$$+ (1 - \omega)n^2 \Theta^4 + \frac{\omega}{2} \sum_{m'=1}^M \psi^{m'}\Phi^{m',m}w^{m'} \tag{13}$$

$$\psi_0^m = \varepsilon_0 n_0^2 \Theta_0^4 + 2(1 - \varepsilon_0) \sum_{\mu^{m'}<0} \psi_0^{m'}|\mu^{m'}|w^{m'} \quad, \mu^m > 0 \tag{14a}$$

$$\psi_L^m = \varepsilon_L n_L^2 \Theta_L^4 + 2(1 - \varepsilon_L) \sum_{\mu^{m'}>0} \psi_L^{m'}|\mu^{m'}|w^{m'} \quad, \mu^m < 0 \tag{14b}$$

where the dimensionless temperature Θ, the dimensionless axial coordinate X, the dimensionless derivative of refractive index γ, the dimensionless radiative intensity ψ, the conduction–radiation parameter N_{cr}, the optical thickness τ_L, and the scattering albedo ω, are defined as following:

$$\Theta = \frac{T}{T_{ref}}, \quad X = x/L, \quad \gamma = \frac{1}{\tau_L}\left(\frac{1}{n}\frac{dn}{dX} \right), \quad \psi = \frac{\pi I}{\sigma T_{ref}^4},$$

$$N_{cr} = \frac{\kappa \beta}{4\sigma T_{ref}^3}, \quad \tau_L = \beta L, \quad \omega = \frac{k_s}{\beta} \tag{15}$$

where T_{ref} is the reference temperature.

Eq. (13) for $m = 1, 2, \ldots, M$ will not be iteratively solved based on finite volume method as the conventional way in Refs. [36–38]. As in Ref. [39], the strategy of the RTE discretization in this article belongs to the category of so-called space-angle decoupling.

First, the mapping of arbitrary interval $x \in [X_1, X_2]$ to standard interval $s \in [-1, 1]$ is needed to fit the requirement of Chebyshev polynomial

$$s = \frac{2x - (X_2 + X_1)}{X_2 - X_1}, \quad x = \frac{s(X_2 - X_1) + (X_2 + X_1)}{2} \tag{16}$$

After mapping, the dimensionless RTE and energy equation become

$$\left[\frac{\mu^m}{\tau_L}\left(\frac{2}{X_2 - X_1} \right)\frac{\partial}{\partial s} + \frac{\gamma}{w^m}\max\left(\alpha^{m+1/2}, 0\right) + \frac{\gamma}{w^m}\max\left(-\alpha^{m-1/2}, 0\right) + 1 \right]$$

$$\psi^m = \frac{\gamma}{w^m}\max\left(-\alpha^{m+1/2}, 0\right)\psi^{m+1} + \frac{\gamma}{w^m}\max\left(\alpha^{m-1/2}, 0\right)\psi^{m-1}$$

$$+ (1 - \omega)n^2 \Theta^4 + \frac{\omega}{2} \sum_{m'=1}^M \psi^{m'}\Phi^{m',m}w^{m'} \tag{17}$$

$$\left(\frac{2}{X_2 - X_1} \right)^2 \frac{\partial^2 \Theta}{\partial s^2} = \frac{\tau_L^2}{N_{cr}}(1 - \omega)\left(n^2 \Theta^4 - \frac{1}{2} \sum_{m=1}^M \psi^m w^m \right) \tag{18}$$

The Gauss–Lobatto collocation points are used for spatial discretization

$$s_i = -\cos\frac{\pi i}{N}, \quad i = 0, 1, \ldots, N \tag{19}$$

The dimensionless unknown radiative intensity and temperature can be approximated by Chebyshev polynomial as

$$\psi_N^m(s) = \sum_{k=0}^N \hat{\psi}_k^m T_k(s) \tag{20}$$

$$\Theta_N(s) = \sum_{k=0}^N \hat{\Theta}_k T_k(s) \tag{21}$$

where $\psi_N^m(s) \approx \psi^m(s)$, $\Theta_N(s) \approx \Theta(s)$, the coefficients $\hat{\psi}_k^m$ and $\hat{\Theta}_k$ are determined by the collocation points s_k, $k = 0, 1, \ldots, N$; and the $T_k(s)$ is the first kind Chebyshev polynomial. The polynomial of degree N defined by Eqs. (20) and (21) can be the Lagrange interpolation polynomial based on the set $\{s_i\}$ like

$$\psi_N^m(s) = \sum_{j=0}^N h_j(s)\psi^m(s_j) \tag{22}$$

$$\Theta_N(s) = \sum_{j=0}^N h_j(s)\Theta(s_j) \tag{23}$$

where $h_j(s)$ is a function of the first order derivative of Chebyshev polynomial.

To avoid spectral coefficients solution and fast cosine transformation, we use Eqs. (22) and (23) rather than Eqs. (20) and (21) in Eqs. (17) and (18).

Substituting Eq. (22) into Eq. (17), one can obtain the spectral discretized algebraic equations

$$(\mathbf{A}^m + \mathbf{B}^m)\boldsymbol{\psi}^m = \mathbf{F}^m \tag{24}$$

where the elemental expressions for matrix $\mathbf{A}^m$, $\mathbf{B}^m$ and $\mathbf{F}^m$ are

$$A_{ik}^m = \frac{\mu^m}{\tau_L}\left(\frac{2}{X_2 - X_1}\right)D_{s,ik}^{(1)}$$

$$B_{ik}^m = \begin{cases} \frac{\gamma(s_i)}{w^m}\max\left(\alpha^{m+1/2}, 0\right) + \frac{\gamma(s_i)}{w^m}\max(-\alpha^{m-1/2}, 0) + 1, & i = k \\ 0, & \text{otherwise} \end{cases}$$

$$F_i^m = \frac{\gamma(s_i)}{w^m}\max\left(-\alpha^{m+1/2}, 0\right)\psi^{m+1}(s_i) + \frac{\gamma(s_i)}{w^m}\max\left(\alpha^{m-1/2}, 0\right)\psi^{m-1}(s_i)$$
$$+ (1-\omega)n^2(s_i)\Theta^4(s_i) + \frac{\omega}{2}\sum_{m'=1}^{M}\psi^{m'}(s_i)\Phi^{m',m}w^{m'}$$

and the $\mathbf{D}_s^{(1)}$ is the first order derivative matrix in s direction corresponding to Gauss–Lobatto collocation points and its detailed computation can be found in Ref. [15].

Boundary conditions, given by Eqs. (14a) and (14b), must be imported before solving Eq. (24). For the Dirichlet boundary condition, it can be easily imported and the detail can be found in [13–15,40].

Eq. (18) is a strong non-linear partial differential equation. To reduce the nonlinearity of Eq. (18), we tried to rearrange it as

$$\left(\frac{2}{X_2 - X_1}\right)^2\frac{\partial^2\Theta}{\partial s^2} - \frac{2(1-\omega)\tau_L^2}{N_{cr}}n^2\Theta^4$$
$$= -\frac{\tau_L^2}{N_{cr}}(1-\omega)\left(n^2\Theta^4 + \frac{1}{2}\sum_{m=1}^{M}\psi^m w^m\right) \tag{25}$$

Similarly, the spectral discretization of energy equation can be written in matrix form

$$\mathbf{P}\boldsymbol{\Theta} = \mathbf{V} \tag{26}$$

where the elemental expressions for matrix $\mathbf{P}$, and $\mathbf{V}$ are

$$P_{ik} = \begin{cases} \left(\frac{2}{X_2 - X_1}\right)D_{s,ik}^{(2)} - \frac{2(1-\omega)\tau_L^2}{N_{cr}}n^2(s_i)[\Theta^*(s_i)]^3, & i = K \\ \left(\frac{2}{X_2 - X_1}\right)D_{s,ik}^{(2)}, & \text{otherwise} \end{cases}$$

$$V_i = -\frac{\tau_L^2}{N_{cr}}(1-\omega)\left\{n^2(s_i)[\Theta^*(s_i)]^4 + \frac{1}{2}\sum_{m=1}^{M}\psi^m(s_i)w^m\right\}$$

where the superscript "*" of dimensionless temperature Θ denotes the last iterative value, and the matrix $\mathbf{D}_s^{(2)}$ is the second order derivative matrix in s direction corresponding to Gauss–Lobatto collocation points. Boundary conditions, given by Eqs. (12a) and (12b), must be imported before solving Eq. (26).

The implementation of Chebyshev collocation spectral method for solving combined radiation and conduction heat transfer in graded index medium can be executed through the following routine:

Step1: Choose the resolution N and compute the coordinate values of nodes, hence compute the derivative of refractive index $\gamma(s)$ at nodes.
Step 2: Choose the direction number M and the corresponding direction cosine, as well as the weights w^m, hence compute the angular difference constants α.

Step 3: Give dimensionless radiative intensity ψ^m and dimensionless temperature Θ initial assumptions (zero for example) in all directions and all nodes except for boundaries.
Step 4: Start iteration in each angular direction for $m = 1, 2, \ldots, M$, and assemble matrices $\mathbf{A}^m$, $\mathbf{B}^m$ and $\mathbf{F}^m$. Import Dirichlet boundary conditions and solve the discretized RTE Eq. (24) to update the dimensionless radiative intensity ψ^m field of each direction.
Step 5: Assemble the matrices $\mathbf{P}$ and $\mathbf{V}$, import Dirichlet boundary conditions and solve the discretized energy Eq. (26) to update the dimensionless temperature.
Step 6: Terminate the iteration if the maximum absolute difference of the last and present dimensionless radiative intensity or temperature is less than the tolerance (10^{-12} for example), otherwise go back to step 4.

3. Results and discussion

To verify the Chebyshev collocation spectral method for combined radiation and conduction heat transfer in one-dimensional semitransparent medium with graded index, three various test cases are adopted. For the following numerical study, the temperature of boundary walls are imposed as $T_0 = 1000$ K and $T_L = 1500$ K, the reference temperature is $T_{ref} = 1000$ K, and the thickness of the slab keeps a constant value of 1 cm.

3.1. Case 1: one-dimensional non-scattering gray medium with linear refractive index

In this case, we consider the combined radiation and conduction heat transfer in an absorbing–emitting medium with linear refractive index. The dimensionless temperature distributions obtained by SP-DOM are plotted in Fig. 2 for the case of $\tau_L = 1.0$, $N_{cr} = 0.04409$ and $\varepsilon_0 = \varepsilon_L = 1.0$, and have been validated against available results in Ref. [7]. In this literature, Huang employ the pseudo-source adding method in combination with the curved ray tracing technique (PSA-CRT). Here, a resolution (number of nodes) of 19 is used for spatial discretization in our work, however, 100 nodes are used in Ref. [7] for PSA-CRT method. As shown in Fig. 2, the results of the SP-DOM match very well with those of Huang for different emissivities of boundary walls. In general, the maximum relative error between these results is less than 1.1%.

The dimensionless radiative heat flux distributions are shown in Fig. 3 for the case of $\tau_L = 10.0$, $N_{cr} = 4.40917$, $\varepsilon_0 = 1.0$ and $\varepsilon_L = 0.2$,
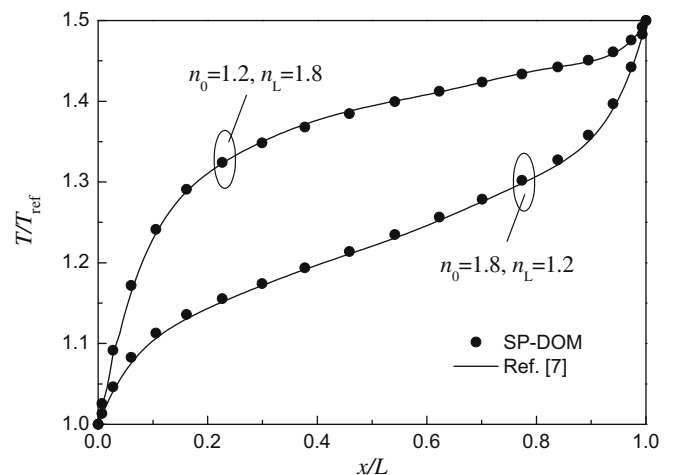
Fig. 2. Dimensionless temperature distributions in the case of $\tau_L = 1.0$, $N_{cr} = 0.04409$ and $\varepsilon_0 = \varepsilon_L = 1.0$.
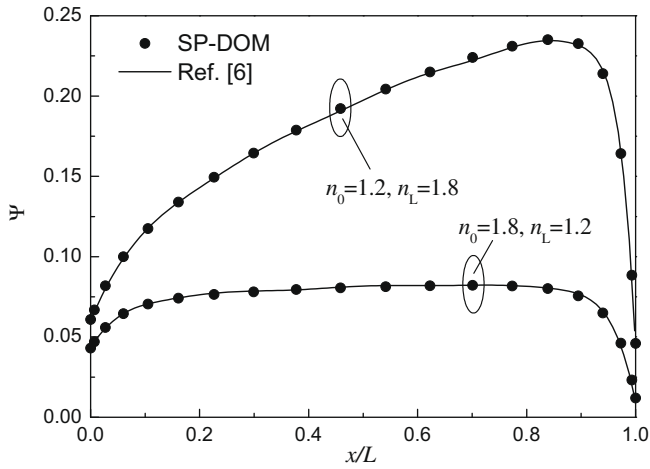
Fig. 3. Dimensionless radiative heat flux distributions in the case of $\tau_L = 10.0$, $N_{cr} = 4.40917$, $\varepsilon_0 = 1.0$ and $\varepsilon_L = 0.2$.

Fig. 4. The exponential convergence rate of the spectral method according to total number of solution nodes.

but with two combinations of n_0 and n_L. The dimensionless radiative heat flux is defined by

$$\Psi = \left[2\pi \int_{-1}^{1} I\mu \, d\mu \right] \Big/ \left[n_0^2 \sigma (T_0^4 - T_L^4) \right] \tag{27}$$

For the purpose of comparison, the results obtained by Xia et al. which are based on PSA-CRT method from Ref. [6] are copied. Again, the SP-DOM results agree very well with them.

The exponential convergence characteristics of spectral methods [13] for the solution of dimensionless temperature distribution for different values of conduction–radiation parameter are studied. Now, for the sake of quantitative comparison with the benchmark solution, the integral averaged relative error of spectral methods is defined as

Integra averaged relative error

$$= \frac{\int |\text{spectra methods solution}\,(x) - \text{benchmark results}\,(x)|\,dx}{\int |\text{benchmark results}\,(x)|\,dx} \times 100\% \tag{28}$$

Fig. 4 shows the exponential convergence characteristics of spectral methods against the resolution for the case of $n(x) = 1.2 + 0.6(x/L)$, $\tau_L = 1.0$, and $\varepsilon_0 = \varepsilon_L = 1.0$, where the solution obtained using $N=21$ is considered as the benchmark solution. It can be seen that the convergence rate is very fast for different values of conduction–radiation parameter and approximately follows the exponential law. With the increase of conduction–radiation parameter, the convergence rate tends to increase.

The effects of various combinations of resolutions and angular directions on numerical solutions under the case of $n(x) = 1.2 + 0.6(x/L)$, $\tau_L = 1.0$, $N_{cr} = 0.04409$ and $\varepsilon_0 = \varepsilon_L = 1.0$, are shown in Fig. 5. Clearly, the combination of $N=11$ and $M=4$ almost gives the same smooth solution as the combination of $N=51$ and $M=12$ does. The convergent characteristic of spectral methods is demonstrated again in this article.

3.2. Case 2: one-dimensional non-scattering gray medium with sinusoidal refractive index

In this case, a sinusoidal refractive index is studied. The SP-DOM approach is used to solve the distribution of temperatures and radiative heat fluxes in the slab. In Fig. 6, results of the SP-DOM have been validated against those available in Ref. [10]. Again, a resolution of 19 is used for spatial discretization; however, 101 nodes are used in Ref. [10] for MPLG method. Comparisons of the dimensionless temperature Θ results for $n(x) = 1.8 - 0.6 \sin(\pi x/L)$,
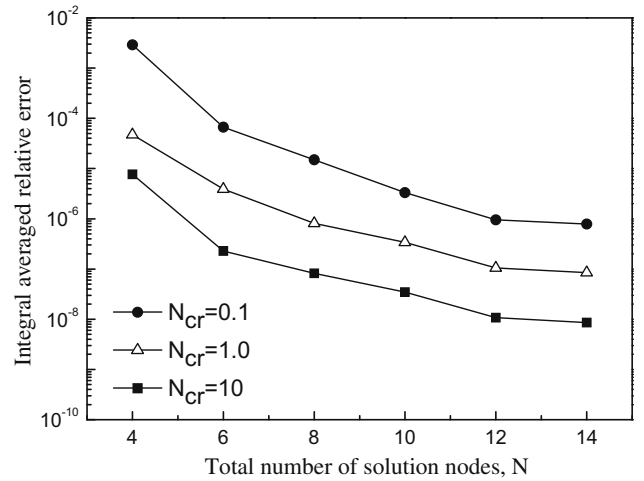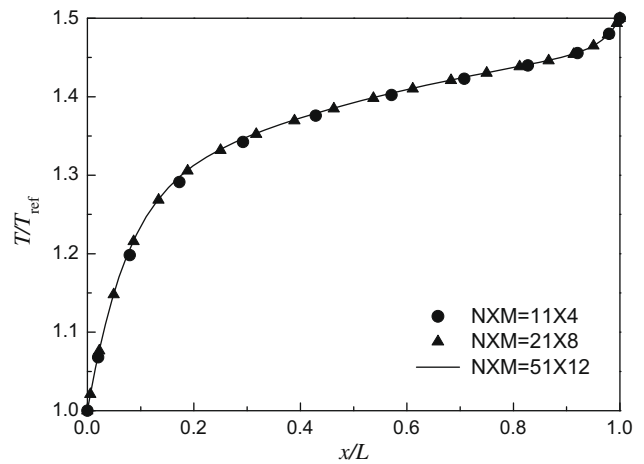

Fig. 5. Effects of resolution and angular discretization in the case of $\tau_L = 1.0$, $N_{cr} = 0.04409$, $n_0 = 1.2$, $n_L = 1.8$ and $\varepsilon_0 = \varepsilon_L = 1.0$.

$\tau_L = 1.0$ and $N_{cr} = 0.04409$ with different boundary conditions are made in Fig. 6. From Fig. 6, the results of SP-DOM match very well with those of Liu et al. [10] by MPLG, and the maximum rela-
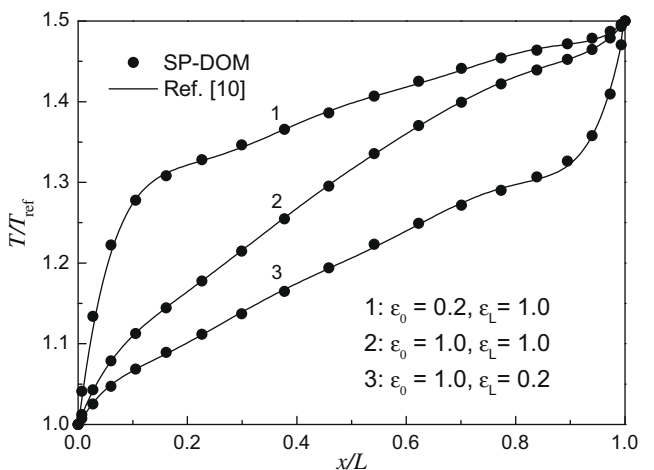

Fig. 6. Dimensionless temperature distributions in the case of $n(x) = 1.8 - 0.6 \sin(\pi x/L)$, $\tau_L = 1.0$ and $N_{cr} = 0.04409$.
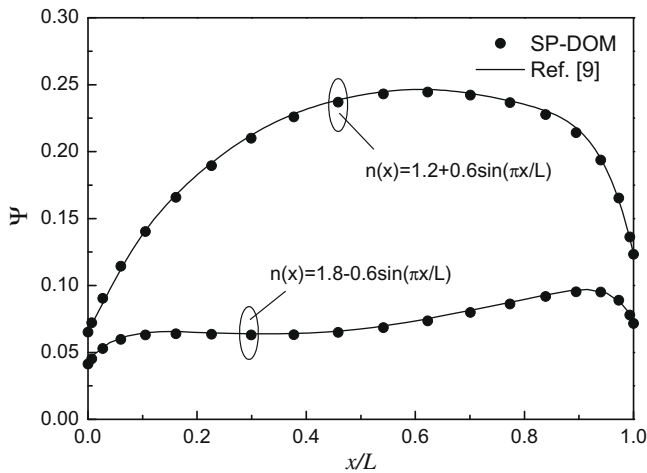
Fig. 7. Dimensionless radiative heat flux distributions in the case of $\tau_L = 10.0$, $N_{cr} = 4.40917$ and $\varepsilon_0 = \varepsilon_L = 1.0$.

tive error of SP-DOM for the dimensionless temperature is less than 1.41%.

The dimensionless radiative heat flux distribution obtained by SP-DOM is plotted in Fig. 7 in the case of $\tau_L = 10.0$, $N_{cr} = 4.40917$ and $\varepsilon_0 = \varepsilon_L = 1.0$. Those results by MPLG are copied from Ref. [10] again for comparison. As shown in Fig. 7, the maximum relative error of dimensionless radiative heat fluxes is less than 1% with respect to the results of Ref. [10].

3.3. Case 3: one-dimensional isotropically scattering gray medium with linear refractive index

In this case, we consider the combined radiation and conduction heat transfer in an isotropically scattering gray medium with linear refractive index.

The dimensionless temperature distributions by SP-DOM within the slab are shown in Fig. 8 for different refractive indices, namely, $n(x) = 1.2 + 0.6(x/L)$ and $n(x) = 1.8 - 0.6(x/L)$. In this case, the optical thickness is $\tau_L = 10.0$ the conduction–radiation parameter is $N_{cr} = 0.44092$, the wall emissivities are $\varepsilon_0 = 0.2$ and $\varepsilon_L = 1.0$, and the scattering albedo is $\omega = 0.9$. This case was also used as a test case by Yi et al. [11] in which the discrete curved

Fig. 8. Dimensionless temperature distributions in the case of $\tau_L = 10.0$, $N_{cr} = 0.44092$, $\varepsilon_1 = 0.2$, $\varepsilon_2 = 1.0$ and $\omega = 0.9$.
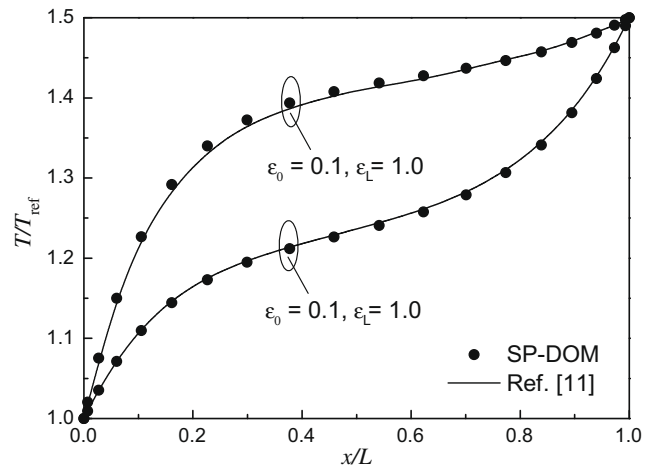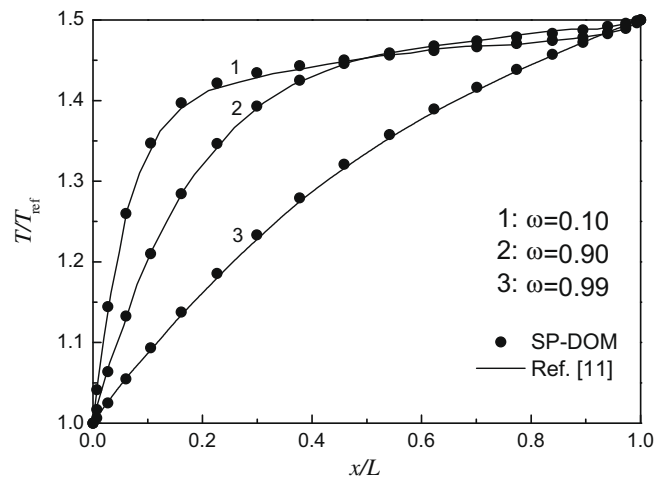

Fig. 9. Dimensionless temperature distributions in the case of $n_0 = 1.8$, $n_L = 1.2$, $\tau_L = 1.0$, $N_{cr} = 0.04409$ and $\omega = 0.9$.

Fig. 10. Dimensionless temperature distributions in the case of $n_0 = 1.2$, $n_L = 1.8$, $\tau_L = 1.0$, $N_{cr} = 0.04409$, $\varepsilon_0 = 0.2$ and $\varepsilon_L = 1.0$.
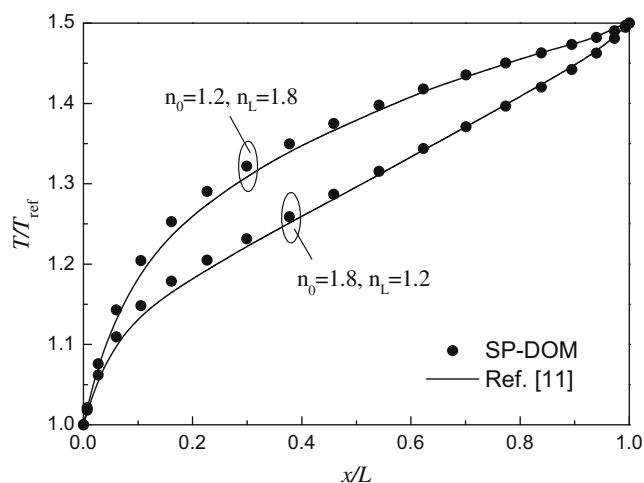
ray tracing method was used. Same as above, a resolution of 19 is used for spatial discretization in our work, however, 100 nodes are used in Ref. [11] for their discrete curved ray tracing method. As shown in Fig. 8, the SP-DOM results agree with those obtained by Yi et al. very well. The maximum relative error of our results is less than 2% with respect to the values of Ref. [11].

The dimensionless temperature distributions by SP-DOM within the slab are plotted in Fig. 9 for the case of $n(x) = 1.8 - 0.6(x/L)$, $\tau_L = 1.0$, $N_{cr} = 0.04409$ and $\omega = 0.9$, and compared to the results obtained by Yi et al.[11]. The results by SP-DOM are very close to those obtained by Yi et al.

The dimensionless temperature distributions by SP-DOM are plotted in Fig. 10 for different scattering albedo, namely, $\omega = 0.1$, $\omega = 0.9$ and $\omega = 0.99$. For this case, the refractive index $n(x) = 1.2 + 0.6(x/L)$, the optical thickness is $\tau_L = 1.0$, the conduction–radiation parameter is $N_{cr} = 0.04409$, the wall emissivities are $\varepsilon_0 = 0.2$ and $\varepsilon_L = 1.0$. In Ref. [11], Yi et al. employed the discrete curved ray tracing method. For the case of small scattering albedo and very strong scattering, no observable difference could be detected between the results by SP-DOM and discrete curved ray tracing method when they are presented in graphical form.

4. Conclusions

The Chebyshev collocation spectral method is employed to solve combined radiation and conduction heat transfer in one-dimensional semitransparent medium with graded index. Both the radiative heat transfer and energy equation are discretized using Chebyshev collocation points in space. The numerical results for typical cases verified that the Chebyshev collocation spectral method can provide exponential convergence. Compared with the other approximate solutions, such as, PSA-CRT, MLPG, and discrete curved ray tracing method, from the formulations and implementations we can conclude that the present method, SP-DOM so called, have good accuracy and high efficiency in solving the combined radiation and conduction heat transfer in one-dimensional semitransparent graded index medium.

Acknowledgement

References

[1] R. Siegel, J.R. Howell, Thermal Radiation Heat Transfer, fourth ed., Taylor & Francis, New York, 2002.

[2] M. Born, E. Wolf, Principles of Optics, Seventh ed., Cambridge University Press, New York, 1999.

[3] Y.T. Qiao, Graded Index Optics, Science Press, Beijing, 1991.

[4] R. Siegel, C.M. Spuckler, Variable refractive index effects on radiation in semitransparent scattering multilayered regions, J. Thermophys Heat Transfer 7 (4) (1993) 624–630.

[5] P. Ben Abdallah, V. Le Dez, Radiative flux field inside an absorbing–emitting semi-transparent slab with variable spatial refractive index at radiative conductive coupling, J. Quant. Spectrosc. Radiat. Transfer 67 (2) (2000) 125–137.

[6] X.L. Xia, Y. Huang, H.P. Tan, X.B. Zhang, Simultaneous radiation and conduction heat transfer in a graded index semitransparent slab with gray boundaries, Int. J. Heat Mass Transfer 45 (13) (2002) 2673–2688.

[7] Y. Huang, A study on the thermal radiative transfer in gradient index semitransparent medium. Ph.D. Dissertation, Harbin Institute of Technology, Harbin, People's Republic of China, 2002.

[8] Y. Huang, X.L. Xia, H.P. Tan, Coupled radiation and conduction in a graded index layer with specular surfaces, J. Thermophys Heat Transfer 18 (2) (2004) 281–285.

[9] L.H. Liu, H.P. Tan, Transient temperature response in semitransparent variable refractive index medium subjected to a pulse irradiation, J. Quant. Spectrosc. Radiat. Transfer 83 (3–4) (2004) 333–344.

[10] L.H. Liu, J.Y. Tan, B.X. Li, Meshless approach for coupled radiative and conductive heat transfer in one-dimensional graded index medium, J. Quant. Spectrosc. Radiat. Transfer 101 (2) (2006) 237–248.

[11] H.L. Yi, H.P. Tan, J.F. Luo, S.K. Dong, Effects of graded refractive index on steady and transient heat transfer inside a scattering semitransparent slab, J. Quant. Spectrosc. Radiat. Transfer 96 (3–4) (2005) 363–381.

[12] H.P. Tan, H.L. Yi, J.F. Luo, H.C. Zhang, Transient coupled heat transfer inside a scattering medium with graded refractive index, J. Thermophys Heat Transfer 20 (3) (2006) 583–594.

[13] D. Gottlieb, S.A. Orszag, Numerical analysis of spectral methods: theory and applications, in: Regional Conference Series in Applied Mathematics, SIAM, Philadelphia, PA, vol. 28, 1977, pp. 1–168.

[14] C. Canuto, M.Y. Hussaini, A. Quarteroni, T.A. Zang, Spectral Methods in Fluid Dynamics, Springer, New York, 1988.

[15] R. Peyret, Spectral Methods for Incompressible Viscous Flow, Springer, New York, 2002.

[16] F.B. Belgacem, M. Grundmann, Approximation of the wave and electromagnetic diffusion equations by spectral methods, SIAM J. Sci. Comput. 20 (1) (1998) 13–32.

[17] X.W. Shan, D. Montgomery, H.D. Chen, Nonlinear magnetohydrodynamics by Galerkin-method computation, Phys. Rev. A 44 (10) (1991) 6800–6818.

[18] M. Zenouzi, Y. Yener, Simultaneous radiation and natural convection in vertical slots, Am. Soc. Mech. Eng., Heat Transfer Div. (Publ.) HTD 203 (1992) 179–186.

[19] M. Zenouzi, Y. Yener, Thermal stability of a radiating fluid in a vertical narrow slot, Am. Soc. Mech. Eng., Heat Transfer Div. (Publ.) HTD 219 (1992) 1–7.

[20] D.C. Kuo, J.C. Morales, K.S. Ball, Combined natural convection and volumetric radiation in a horizontal annulus: spectral and finite volume predictions, Am. Soc. Mech. Eng., Heat Transfer Div. (Publ.) HTD 324 (1996) 29–36.

[21] D.C. Kuo, J.C. Morales, K.S. Ball, Combined natural convection and volumetric radiation in a horizontal annulus: spectral and finite volume predictions, J. Heat Transfer 121 (3) (1999) 610–615.

[22] B. Ganz, P. Schmittel, R. Koch, S. Wittig, Validation of numerical methods at a confined turbulent natural gas diffusion flame considering detailed radiative transfer, in: American Society of Mechanical Engineers (Paper), GT: 9, 1998.

[23] J.V.P. De Oliveira, A.V. Cardona, M.T. Vilhena, R.C. Barros, A semi-analytical numerical method for time-dependent radiative transfer problems in slab geometry with coherent isotropic scattering, J. Quant. Spectrosc. Radiat. Transfer 73 (1) (2002) 55–62.

[24] F.E. Lara, M. Rieutord, The dynamics of a fully radiative rapidly rotating star enclosed within a spherical box, Astron. Astrophys. 470 (3) (2007) 1013–1022.

[25] M.F. Modest, J. Yang, Elliptic PDE formulation and boundary conditions of the spherical harmonics method of arbitrary order for general three-dimensional geometries, J. Quant. Spectrosc. Radiat. Transfer 109 (9) (2008) 1641–1666.

[26] B. Ritchie, P.G. Dykema, D. Braddy, Use of fast-Fourier-transform computational methods in radiation transport, Phys. Rev. E 56 (2) (1997) 2217–2227.

[27] A.D. Kim, A. Ishimaru, A Chebyshev spectral method for radiative transfer equations applied to electromagnetic wave propagation and scattering in a discrete random medium, J. Comput. Phys. 152 (1) (1999) 264–280.

[28] A.D. Kim, M. Moscoso, Chebyshev spectral methods for radiative transfer, SIAM J. Sci. Comput. 23 (6) (2002) 2074–2094.

[29] A.D. Kim, M. Moscoso, Radiative transfer computations for optical beams, J. Comput. Phys. 185 (1) (2003) 50–60.

[30] N. Aouled-Dlala, T. Sghaier, E. Seddiki, Numerical solution of radiative and conductive heat transfer in concentric spherical and cylindrical media, J. Quant. Spectrosc. Radiat. Transfer 107 (3) (2007) 443–457.

[31] B.W. Li, Y.S. Sun, Y. Yu, Iterative and direct Chebyshev collocation spectral methods for one-dimensional radiative heat transfer, Int. J. Heat Mass Transfer 51 (25–26) (2008) 5887–5894.

[32] Y.S. Sun, B.W. Li, Chebyshev collocation spectral method for one dimensional radiative heat transfer in graded index media, Int. J. Therm. Sci. 48 (4) (2009) 691–698.

[33] B.W. Li, Y.S. Sun, D.W. Zhang, Chebyshev collocation spectral methods for coupled radiation and conduction in a concentric spherical participating medium, J. Heat Transfer 131 (6) (2009) 062701–062709.

[34] D. Lemonnier, V. Le Dez, Discrete ordinates solution of radiative transfer across a slab with variable refractive index, J. Quant. Spectrosc. Radiat. Transfer 73 (2–5) (2002) 195–204.

[35] M.F. Modest, Radiative Heat Transfer, second ed., Academic Press, San Diego, CA, 2003.

[36] W.A. Fiveland, Discrete-ordinates solutions of the radiative transport equation for rectangular enclosures, Trans. ASME J. Heat Transfer 106 (4) (1984) 699–706.

[37] W.A. Fiveland, Discrete ordinate methods for radiative heat transfer in isotropically and anisotropically scattering media, Trans. ASME J. Heat Transfer 109 (3) (1987) 809–812.

[38] W.A. Fiveland, Three-dimensional radiative heat-transfer solutions by the discrete-ordinates method, J. Thermophys Heat Transfer 2 (4) (1988) 309–316.

[39] J.P. Pontaza, J.N. Reddy, Least-squares finite element formulations for one-dimensional radiative transfer, J. Quant. Spectrosc. Radiat. Transfer 95 (3) (2005) 387–406.

[40] J.P. Boyd, Chebyshev & Fourier Spectral Methods, second ed., Dover, New York, 2001.